Journal of Solid State Chemistry 184 (2011) 2293–2298

Contents lists available at ScienceDirect

Journal of Solid State Chemistry

journal homepage: www.elsevier.com/locate/jssc

Crystal growth, structures, and optical properties of the cubic double perovskites Ba_2MgWO_6 and Ba_2ZnWO_6

Daniel E. Bugaris [a], Jason P. Hodges [b], Ashfia Huq [b], Hans-Conrad zur Loye [a,*]

[a] Department of Chemistry and Biochemistry, University of South Carolina, Columbia, SC 29208, USA
[b] Neutron Scattering Science Division, Oak Ridge National Laboratory, Oak Ridge, TN 37831, USA

ARTICLE INFO

Article history:
Received 12 May 2011
Received in revised form
14 June 2011
Accepted 19 June 2011
Available online 1 July 2011

Keywords:
Tungstate
Crystal growth
Crystal structure
Neutron diffraction
Luminescence

ABSTRACT

Single crystals of the tungstates Ba_2MgWO_6 and Ba_2ZnWO_6 have been grown for the first time. The crystals were prepared with molten potassium carbonate acting as a flux. According to the single-crystal X-ray diffraction structure determination, the compounds crystallize in space group $Fm\bar{3}m$ of the cubic system with a double perovskite structure, $A_2BB'O_6$. These structural findings were confirmed with neutron diffraction on polycrystalline samples synthesized by a high-temperature solid-state route. Both sets of diffraction data reveal that the M^{2+} and W^{6+} cations are fully ordered on the *B* and *B′* sites. Ba_2MgWO_6 and Ba_2ZnWO_6 exhibit room-temperature luminescence with green and yellow emissions, respectively.

1. Introduction

Tungstates possessing the double perovskite structure ($A_2BB'O_6$) have been investigated since the 1950s [1–6]. The electronic structure of these materials has been characterized experimentally, by diffuse reflectance and Raman spectroscopy, and computationally, by density functional theory [7,8]. Furthermore, the dielectric properties of the tungstates have been measured to determine their potential as ceramic materials for microwave applications [9,10].

Despite this interest in tungstate double perovskites, little structural characterization has been performed beyond powder X-ray diffraction. Neutron diffraction has been conducted on polycrystalline samples of phases with magnetic *B* cations, such as Ba_2MnWO_6 [11], Sr_2CoWO_6 [12], Ba_2CoWO_6 [13], Ca_2NiWO_6 [14], Ba_2NiWO_6 [13], and Ba_2CuWO_6 [15]. However, to the best of our knowledge, the only compounds in this family that have been grown as single crystals are Sr_2CaWO_6 [16], Ba_2CoWO_6 [17], and Pb_2CoWO_6 [18], and a single-crystal X-ray structure solution was reported only for Sr_2CaWO_6.

The crystals of Sr_2CaWO_6 were produced by sintering a polycrystalline sample at high temperature, while crystals of Ba_2CoWO_6 and Pb_2CoWO_6 were grown from high-temperature solutions of $BaCl_2$ and PbO, respectively. The current compounds, Ba_2MgWO_6 and Ba_2ZnWO_6, were grown from a K_2CO_3 flux. Potassium carbonate has proven to be an extremely versatile reagent for the flux growth of oxide crystals, as it has previously been used to grow single crystals of oxides containing 1st row transition metals [19], platinum group metals [20,21], rare-earth elements [22], and actinides [23,24]. There are far fewer instances of early 2nd and 3rd row transition metal oxides grown from K_2CO_3 fluxes, including examples such as $K_2(UO_2)_2(MoO_4)O_2$, $K_8(UO_2)_8(MoO_5)_3O_6$ [25], and $K_2(UO_2)_2(WO_5)O$ [26]. In these cases, the potassium carbonate served as a reactive flux, whereby the K^+ cation was incorporated into the final product, as opposed to our compounds, Ba_2MgWO_6 and Ba_2ZnWO_6, which did not incorporate potassium. In this paper, we will discuss the crystal growth conditions for these two compounds, as well as the single-crystal X-ray structure determination, the Rietveld refinement of neutron diffraction data, and some optical properties.

2. Experimental

2.1. Materials

The following reagents were used as obtained: $BaCO_3$ (Alfa Aesar, 99.95%), K_2CO_3 (J.T. Baker), ZnO (Alfa Aesar, 99.99%), and WO_3 (Aldrich, 99.995%). MgO was prepared from the thermal decomposition of $MgCO_3$ (Fisher) at 750 °C overnight.

2.2. Crystal growth

For Ba_2MgWO_6, MgO (0.0806 g, 2.0 mmol), WO_3 (0.4637 g, 2.0 mmol), and $BaCO_3$ (0.2960 g, 1.5 mmol) were ground thoroughly with mortar and pestle and placed in an alumina crucible,

* Corresponding author.
E-mail address: zurloye@mail.chem.sc.edu (H.-C. zur Loye).

0022-4596/$ - see front matter © 2011 Elsevier Inc. All rights reserved.
doi:10.1016/j.jssc.2011.06.015

where the charge was covered with K_2CO_3 (5.0 g, 36 mmol). For Ba_2ZnWO_6, ZnO (0.1627 g, 2.0 mmol), WO_3 (0.2319 g, 1.0 mmol), and $BaCO_3$ (0.3947 g, 2.0 mmol) were ground thoroughly with mortar and pestle and placed in an alumina crucible, where the charge was covered with K_2CO_3 (10 g, 72 mmol). The filled crucibles were covered, placed in a furnace, and heated in air from room temperature to 950 °C for Zn and 1050 °C for Mg. After holding at the reaction temperature for 36 h, the furnaces were cooled at 5 °C/h (Mg) and 15 °C/h (Zn) to 800 °C, at which point the furnace was turned off and allowed to cool to room temperature. The excess potassium carbonate flux was removed by washing with distilled water, aided by sonication, and the faint blue prismatic crystals were isolated by vacuum filtration.

2.3. Solid-state synthesis

Bulk polycrystalline samples of Ba_2MWO_6 (M=Mg, Zn) were prepared by classical solid-state synthesis from a 2:1.1:1 ratio of $BaCO_3$, MgO or ZnO, and WO_3. The 10 mol% excess of MgO and ZnO was employed to suppress the formation of $BaWO_4$ as an impurity. The mixture was thoroughly ground with a mortar and pestle, and loaded into an alumina boat. For Ba_2ZnWO_6, the reaction mixture was heated 5 times at 950 °C for 12 h, as well as one final heating at 1050 °C for 12 h, with intermittent grinding of the sample between heat treatments. In the case of Ba_2MgWO_6, the reaction mixture was heated once at 950 °C for 12 h, followed by 4 times at 1050 °C for 12 h, again with intermittent grinding of the sample. During both syntheses, an additional 5 mol% MgO or ZnO was added to the reaction mixture to account for any evaporative losses.

2.4. Scanning electron microscopy

Single crystals of Ba_2MgWO_6 and Ba_2ZnWO_6 were analyzed by scanning electron microscopy using an FEI Quanta SEM instrument utilized in high vacuum mode. Energy dispersive spectroscopy verified the presence of Ba, Mg or Zn, and W, and within the detection limits of the instrument, confirmed the absence of extraneous elements such as Al or K.

2.5. Single-crystal X-ray diffraction

Single-crystal X-ray diffraction data were collected with the use of graphite-monochromatized Mo$K\alpha$ radiation (λ=0.71073 Å) at 298 K on a Bruker SMART APEX diffractometer. The crystal-to-detector distance was 5.081 cm. Crystal decay was monitored by recollecting 50 initial frames at the end of the data collection. Data were collected by a scan of 0.3° in ω in groups of 606 frames at φ settings of 0°, 90°, 180°, and 270°. The exposure time was 15 s frame^{-1} for Ba_2ZnWO_6 and 20 s frame^{-1} for Ba_2MgWO_6. The collection of intensity data was carried out with the program SMART [27]. Cell refinement and data reduction were carried out with the use of the program SAINT+ [27]. A numerical absorption correction was performed with the use of the program SADABS [27]. The program SADABS was also employed to make incident beam and decay corrections. The structure was solved with the direct methods program SHELXS and refined with the full-matrix least-squares program SHELXL [28]. The final refinement included anisotropic displacement parameters and a secondary extinction correction. Additional experimental details are given in Table 1 and the Supplementary material.

2.6. Powder X-ray diffraction

Powder X-ray diffraction data were collected on a Rigaku DMAX/2100 powder diffractometer using Cu$K\alpha$ radiation (λ=1.54 Å). Data were collected in 0.02° steps over the 2θ range 10–120°.

Table 1
Structure refinement details from single-crystal X-ray diffraction[a].

Empirical formula	Ba_2MgWO_6	Ba_2ZnWO_6
Formula weight	578.84	619.90
a (Å)	8.1046(9)	8.1362(9)
V (Å^3)	532.4(1)	538.6(1)
ρ_c (g cm^{-3})	7.222	7.645
μ (mm^{-1})	36.262	40.071
F(0 0 0)	984	1056
Crystal size (mm)	0.03 × 0.03 × 0.03	0.05 × 0.04 × 0.03
θ_{max} (deg)	31.26	31.01
Reflections collected	2135	2227
Independent reflections	69	69
Goodness-of-fit on F^2	0.904	0.991
$R(F)$[b]	0.0133	0.0096
$R_w(F^2)$[c]	0.0378	0.0416
Largest diff. peak/hole (e Å^{-3})	1.792 and −0.895	0.450 and −0.753

[a] For both structures, the space group is $Fm\bar{3}m$, Z=4, T=298(2) K, and λ=0.71073 A.
[b] $R(F)=\Sigma||F_0|-|F_c||/\Sigma|F_0|$ for $F_0^2 > 2\sigma(F_0^2)$.
[c] $R_w(F_0^2)=[\Sigma[w(F_0^2-F_c^2)^2]/\Sigma wF_0^4]^{1/2}$. For $F_0^2 < 0$, $w^{-1}=\sigma^2(F_0^2)$; for $F_0^2 \geq 0$, $w^{-1}=\sigma^2(F_0^2)+(0.04\times F_0^2)^2$.

Table 2
Structure refinement details from neutron diffraction[a].

Empirical formula	Ba_2MgWO_6		Ba_2ZnWO_6	
Temperature (K)	10	298	10	298
a (Å)	8.08790(2)	8.10335(2)	8.10424(2)	8.12101(2)
V (Å^3)	529.062(4)	532.101(4)	532.276(4)	535.588(5)
R_p (%)	2.29	2.15	2.55	2.42
R_{wp} (%)	2.77	2.33	3.46	3.13
χ^2	4.516	3.173	6.869	5.622

[a] For all four refinements, the space group is $Fm\bar{3}m$ and Z=4.

2.7. Neutron diffraction

Time-of-flight (TOF) powder neutron diffraction data were collected using 2.24 and 2.73 g samples of Ba_2MgWO_6 and Ba_2ZnWO_6, respectively, contained in 6 mm diameter vanadium sample cans at 10 and 298 K. Diffraction profiles of d-spacing range 0.65–4.3 Å were collected using the POWGEN (BL-11A) neutron powder diffractometer at the Spallation Neutron Source at Oak Ridge National Laboratory, Oak Ridge, TN. Rietveld refinements of the data were performed using the GSAS software package and the EXPGUI interface [29,30]. TOF peak-profile function number 3 and the linear interpolation function were used for modeling the diffraction peaks and background.

The Rietveld refinements showed slightly exaggerated ratios of thermal parameters for Mg/Zn versus W. This behavior is probably due to the limited d-spacing range used for collecting TOF data; ideally, the d-spacing range for data collection should have been extended down to d-spacings=0.45 Å or less. The ratio of thermal parameters can be fixed at values corresponding to the ratios seen in the single-crystal X-ray structure solutions; however, this does not alter the crystal structures obtained from the Rietveld refinements. Therefore, we have opted to leave the values of the thermal parameters for the B and B' sites unconstrained in the final refinements. Experimental details are given in Tables 2 and 3.

2.8. UV–visible spectrometry

The diffuse reflectance spectra of polycrystalline samples of Ba_2MgWO_6 and Ba_2ZnWO_6 were obtained using a Perkin Elmer

Table 3
Atomic coordinates and thermal displacement parameters for Ba_2MgWO_6 and Ba_2ZnWO_6. Values from the single-crystal X-ray structure determination are listed first, followed by the values from the Rietveld refinement of the neutron diffraction data (298 K) in italics.

	x	*y*	*z*	U^a
Ba_2MgWO_6				
Ba	0.25	0.25	0.25	0.0069(2); *0.0054(2)*
Mg	0.5	0.5	0.5	0.008(1); *0.0069(5)*
W	0	0	0	0.0060(2); *0.0034(4)*
O	0.2353(5); *0.23804(7)*	0	0	0.0173(6); *0.0050(4)*, *0.0087(2)*, *0.0087(2)*
Ba_2ZnWO_6				
Ba	0.25	0.25	0.25	0.0074(3); *0.0051(3)*
Zn	0.5	0.5	0.5	0.0064(5); *0.0062(5)*
W	0	0	0	0.0049(2); *0.0030(5)*
O	0.2376(4); *0.23697(8)*	0	0	0.0082(5); *0.0044*(4), *0.0090*(3), *0.0090(3)*

[a] For the thermal displacement parameters from the single-crystal X-ray structure determination, $U=U_{eq}$, which is defined as one-third of the trace of the orthagonalized U_{ij} tensor. For the thermal displacement parameters from the Rietveld refinement of the neutron diffraction data, U_{iso} is listed for Ba, Mg/Zn, and W, and U_{11}, U_{22}, and U_{33} are listed for O.

Lambda 35 UV/Vis Scanning Spectrophotometer equipped with an integrating sphere. The spectra were converted from reflectance to absorbance using the Kubelka–Munk function. The optical band gap energy was estimated using the onset of the absorption edge.

2.9. Luminescence

Excitation and emission of Ba_2MgWO_6 and Ba_2ZnWO_6 were obtained using a Perkin Elmer LS 55 Fluorescence Spectrometer. The excitation wavelengths were 230 and 310 nm for Ba_2MgWO_6, and 380 nm for Ba_2ZnWO_6, while the emission wavelengths were 510 nm (Mg) and 550 nm (Zn). All measurements were performed at room temperature using the polycrystalline samples.

3. Results and discussion

3.1. Preparation and phase identification

Single crystals of Ba_2MgWO_6 and Ba_2ZnWO_6 have been grown for the first time. This was accomplished with the aid of a potassium carbonate flux at 950 °C for the Zn compound and 1050 °C for the Mg compound. In both cases, the crystals were faint blue prisms with a diameter typically less than 0.5 mm. The single-crystal X-ray structure refinements showed no evidence of mixing of Mg or Zn and W on the *B* and *B′* sites. Furthermore, the structure solution indicates that all three metal sites are fully occupied.

Due to the low yield of crystals by the flux method, bulk polycrystalline samples for the neutron diffraction and optical measurements were prepared by a standard solid-state route from $BaCO_3$, MgO or ZnO, and WO_3 with multiple heat treatments at 950 and 1050 °C, with intermittent grinding of the sample. This procedure was repeated until the powder X-ray diffraction no longer showed a change in the pattern. Due to the volatility of MgO and ZnO, these reagents were used in a slight excess to prevent the formation of the thermodynamically stable byproduct $BaWO_4$ or alternatively, the double perovskite with a deficient *B*-site ($Ba_2Zn_{0.9}W_{0.95}O_6$) [10]. Unfortunately, a small amount of MgO and ZnO remained as impurities in the final products according to powder X-ray diffraction (see Supplementary information). Ba_2WO_5 was also present as a minor phase in the sample of Ba_2MgWO_6.

The polycrystalline samples of Ba_2MgWO_6 and Ba_2ZnWO_6 were then used for neutron diffraction experiments at room temperature (298 K) and low temperature (10 K). The low temperature measurements were conducted to determine if either phase undergoes a phase transition to lower symmetry, as seen for Sr_2MgWO_6 which is tetragonal ($I4/m$) below 300 °C and cubic ($Fm\bar{3}m$) above [31]. No phase transition was observed for either Ba_2MgWO_6 or Ba_2ZnWO_6; both maintain the cubic space group $Fm\bar{3}m$ down to 10 K. The Rietveld refinements of the neutron diffraction data for Ba_2MgWO_6 and Ba_2ZnWO_6 are given in Figs. 1–4. The refinements of the room-temperature data revealed 5.1(4) wt% of Ba_2WO_5 and 1.51(6) wt% of MgO as impurities in the Ba_2MgWO_6 sample, and 2.3(2) wt% ZnO as an impurity in Ba_2ZnWO_6.

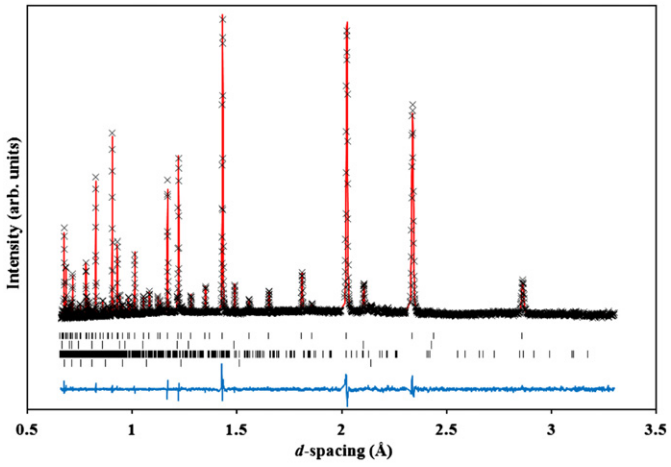

Fig. 1. Rietveld refinement of neutron diffraction data for Ba_2MgWO_6 at low temperature (10 K). Crosses are observed data, the solid red line is the calculated pattern, and the blue line is the difference. Tick marks indicate the allowed Bragg reflections for Ba_2MgWO_6, MgO, Ba_2WO_5, and V (top to bottom). (For interpretation of the references to color in this figure legend, the reader is referred to the web version of this article.)

3.2. Crystal structure

The structural stability of a double perovskite ($A_2BB'O_6$) is determined by the Goldschmidt tolerance factor *t*, where $t=[(r_A+r_O)/\sqrt{2}(0.5r_B+0.5r_{B'}+r_O)]$. For an ideal cubic structure, $t=1$. As the *A* cation becomes too small or the *B* cation too large, the structure distorts by the mechanism of tilting of the *B* and *B′* octahedra. This behavior reduces the crystal symmetry of the double perovskite from cubic to tetragonal and finally to monoclinic, and is reflected in the deviation of the tolerance factor

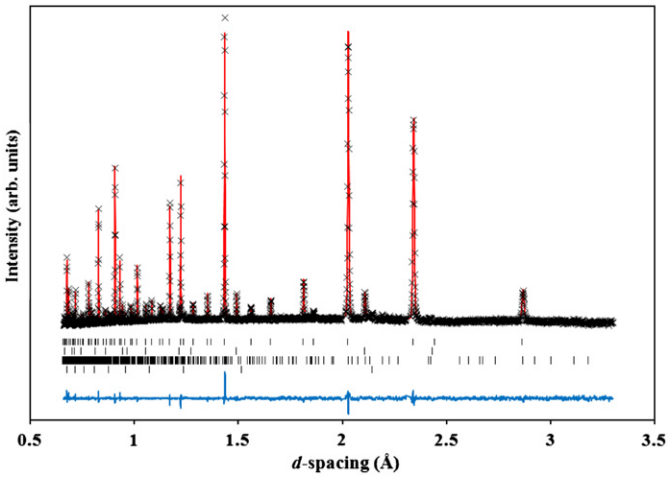

Fig. 2. Rietveld refinement of neutron diffraction data for Ba_2MgWO_6 at room temperature (298 K). Crosses are observed data, the solid red line is the calculated pattern, and the blue line is the difference. Tick marks indicate the allowed Bragg reflections for Ba_2MgWO_6, MgO, Ba_2WO_5, and V (top to bottom). (For interpretation of the references to color in this figure legend, the reader is referred to the web version of this article.)

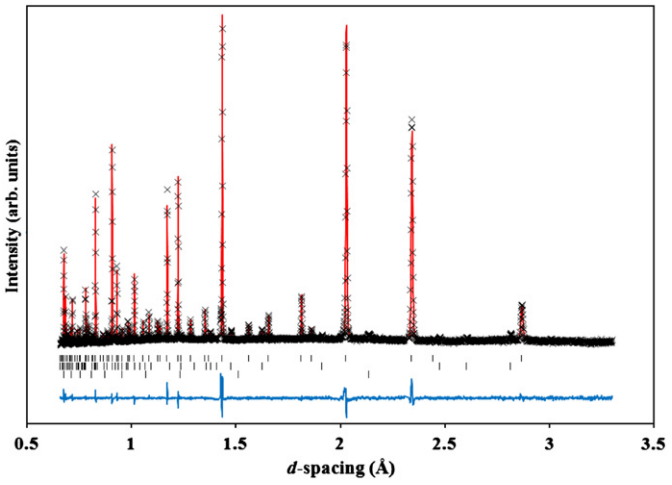

Fig. 3. Rietveld refinement of neutron diffraction data for Ba_2ZnWO_6 at low temperature (10 K). Crosses are observed data, the solid red line is the calculated pattern, and the blue line is the difference. Tick marks indicate the allowed Bragg reflections for Ba_2ZnWO_6, ZnO, and V (top to bottom). (For interpretation of the references to color in this figure legend, the reader is referred to the web version of this article.)

further from unity. The calculated tolerance factors for Ba_2MgWO_6 and Ba_2ZnWO_6 are both $\sim$1.03, which is consistent with the cubic symmetry determined via both single-crystal X-ray and powder neutron diffraction.

Ba_2MgWO_6 and Ba_2ZnWO_6 crystallize in space group $Fm\bar{3}m$ of the cubic crystal system, as verified by both single-crystal X-ray and neutron diffraction. The lattice parameters from the structure refinements are given in Tables 1 and 2. For Ba_2MgWO_6, there is extremely good agreement between the lattice parameters derived from both the single-crystal X-ray data and the neutron data. However, with regards to Ba_2ZnWO_6, there is some discrepancy between the lattice parameters from the single-crystal X-ray and neutron structure solutions. The discrepancy in the lattice parameters may be due to a very slight oxygen deficiency in the single crystals and the corresponding presence of W^{5+}, which would be consistent with the faint blue color

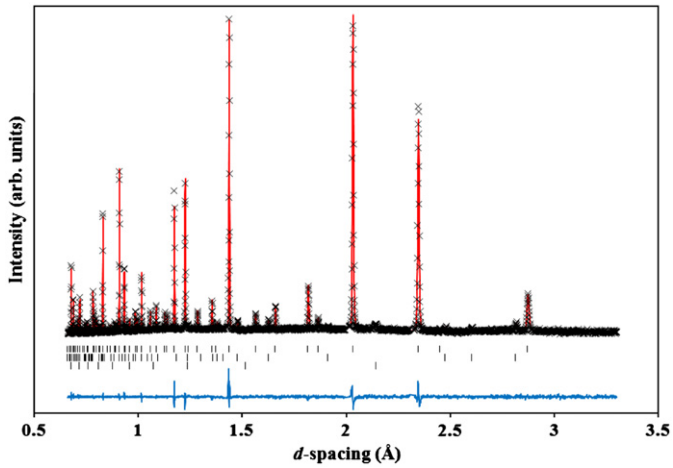

Fig. 4. Rietveld refinement of neutron diffraction data for Ba_2ZnWO_6 at room temperature (298 K). Crosses are observed data, the solid red line is the calculated pattern, and the blue line is the difference. Tick marks indicate the allowed Bragg reflections for Ba_2ZnWO_6, ZnO, and V (top to bottom). (For interpretation of the references to color in this figure legend, the reader is referred to the web version of this article.)

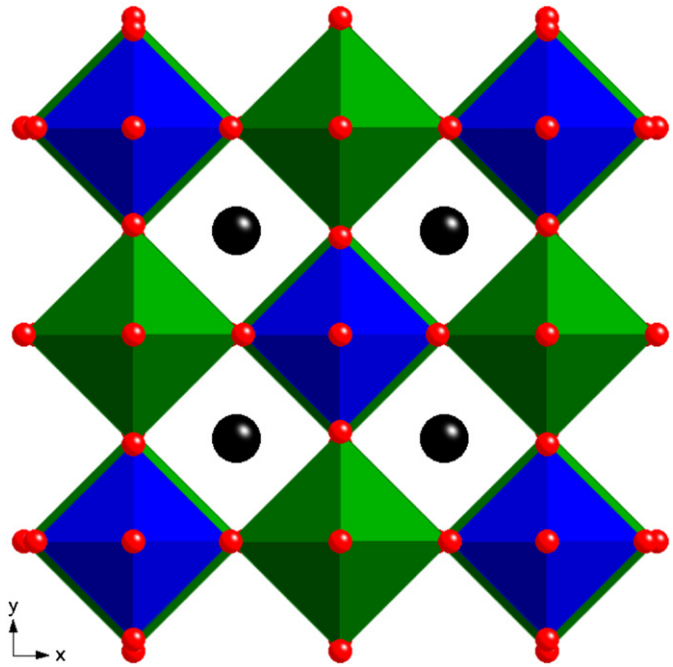

Fig. 5. The crystal structure of Ba_2MWO_6 (M=Mg, Zn). MO_6 octahedra are shown in green, WO_6 octahedra are shown in blue, Ba^{2+} cations are shown in black, and O^{2-} anions are shown in red. (For interpretation of the references to color in this figure legend, the reader is referred to the web version of this article.)

observed. However, this oxygen deficiency would not be detectable in the single-crystal X-ray structure solution as X-rays are relatively insensitive to minor oxygen deficiencies.

Both Ba_2MgWO_6 and Ba_2ZnWO_6 adopt the cubic double perovskite structure with a rock salt lattice of corner-shared octahedra of MgO_6 or ZnO_6 and WO_6, with Ba cations positioned in the cubic 12-fold coordination sites (Fig. 5). As noted earlier, there is no mixing of M and W on the B and B' sites observed in the single-crystal X-ray or neutron structure determinations. This is to be expected due to the large charge difference between the M^{2+} and W^{6+} cations. The bond lengths observed in Ba_2MgWO_6

Table 4
Selected interatomic distances (Å) for Ba_2MgWO_6 and Ba_2ZnWO_6 from both neutron and single-crystal X-ray diffraction data.

Compound	Ba_2MgWO_6			Ba_2ZnWO_6		
Source	Neutron	Neutron	X-ray	Neutron	Neutron	X-ray
T (K)	10	298	298	10	298	298
Ba–O × 12 (Å)	2.86107(2)	2.86665(2)	2.8679(4)	2.86708(2)	2.87316(2)	2.8783(3)
M–O × 6 (Å)	2.1167(6)	2.1228(6)	2.145(4)	2.1277(6)	2.1361(6)	2.135(3)
W–O × 6 (Å)	1.9273(6)	1.9289(6)	1.907(4)	1.9244(6)	1.9244(6)	1.933(3)

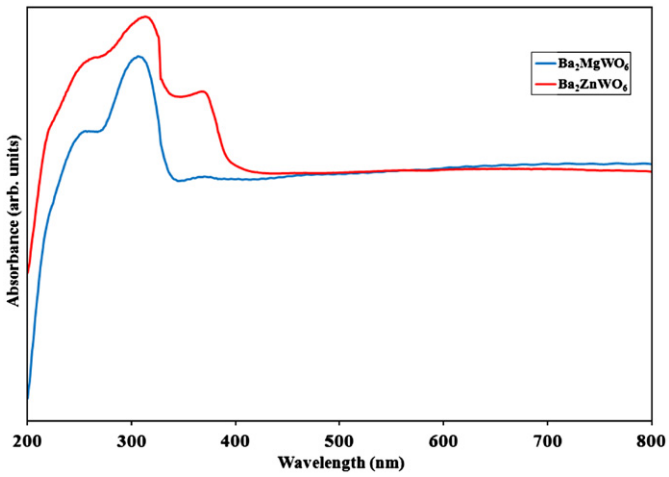

Fig. 6. UV–vis diffuse reflectance spectra of Ba_2MgWO_6 (blue) and Ba_2ZnWO_6 (red). (For interpretation of the references to color in this figure legend, the reader is referred to the web version of this article.)

and Ba_2ZnWO_6 (Table 4) are consistent with those of other similar tungstate perovskite materials. The Ba–O interatomic distances of 2.8679(4) Å in Ba_2MgWO_6 and 2.8783(3) Å in Ba_2ZnWO_6 are comparable to the interatomic distance of 2.8684(6) Å in Ba_2CoWO_6 [32]. The W–O bonds lengths are 1.907(4) Å and 1.933(3) Å in Ba_2MgWO_6 and Ba_2ZnWO_6, respectively, which are similar to the bond lengths in Sr_2CaWO_6, namely 1.90(4)–1.92(2) Å [16].

3.3. Optical properties

The diffuse reflectance UV–visible absorbance spectra for the powder samples of Ba_2MgWO_6 and Ba_2ZnWO_6 are shown in Fig. 6. It has been proposed that the absorption edge in tungstates is due to a charge–transfer transition from the highest filled molecular orbital (the oxygen 2p orbital) to the lowest empty molecular orbital (the tungsten 5d(t_{2g}) orbital) [7]. The UV–visible absorbance spectra display absorption edges at 365 and 355 nm for Ba_2MgWO_6 and Ba_2ZnWO_6, respectively. Estimating the band gap from the onset of the absorption edge yields values approximately equivalent to those reported previously, i.e. 3.4 eV for Ba_2MgWO_6 and 3.5 eV for Ba_2ZnWO_6 [8]. On the basis of these values, these compounds can be classified as wide band gap semiconductors.

The luminescence excitation and emission spectra of Ba_2MgWO_6 and Ba_2ZnWO_6 were collected in order to study the green and yellow emissions, respectively. Optical images of the powders under short UV irradiation (254 nm) for Ba_2MgWO_6 and long UV irradiation (365 nm) for Ba_2ZnWO_6 are shown in Fig. 7. Fig. 8 shows the room temperature excitation and emission spectra for these compounds. The emission peak of the Zn compound has its maximum at 539 nm, with the corresponding

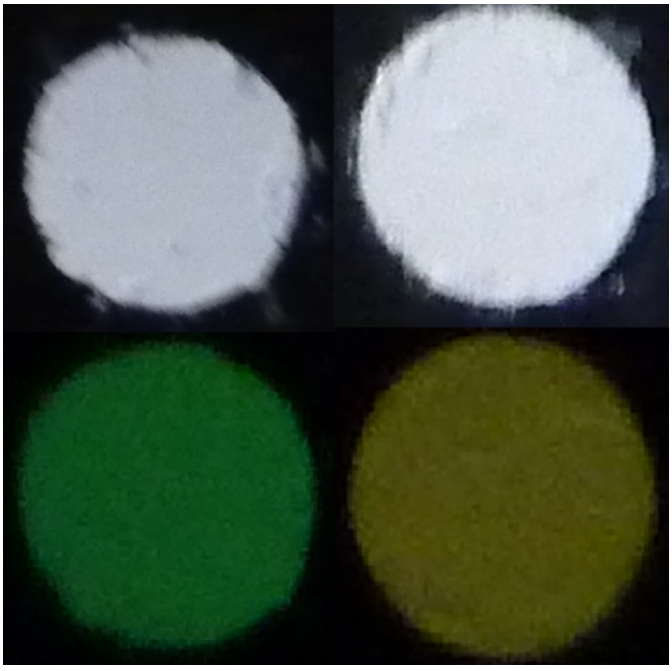

Fig. 7. Optical images of polycrystalline samples of Ba_2MgWO_6 in ambient light (top left) and under 254 nm UV irradiation (bottom left), and Ba_2ZnWO_6 in ambient light (top right) and under 365 nm UV irradiation (bottom right).

excitation maximum at 382 nm. The Mg compound shows the most intense emission at 509 nm with excitation at either 226 or 315 nm (the emission intensity is greater for the 226 nm excitation). For Ba_2MgWO_6, the maximum intensity had previously been reported at 530 nm for an excitation of 254 nm [7], and at 412 and 508 nm for excitations of 277 and 320–340 nm, respectively [33]. The position of our most intense emission for Ba_2MgWO_6 is consistent with that given for the long-wavelength excitation in the second report. Our spectrum of Ba_2MgWO_6 also exhibits a small shoulder at 414 nm, which may correspond to the second emission band reported at 412 nm for short-wavelength excitation. However, unlike the previous report, our emission at 509 nm remains the most intense with either short- or long-wavelength excitation. There is negligible contribution to the luminescence from the impurities, i.e. MgO and Ba_2WO_5 in the Ba_2MgWO_6 sample, and ZnO in the Ba_2ZnWO_6 sample (see Supplementary material).

It is not surprising that these compounds exhibit luminescence, as tungstates are a well-known class of luminescent materials [34,35]. In some instances, tungsten has been deliberately doped into compounds as an activator, such as W^{6+}-Ln_2TeO_6 (Ln=Y, La, Gd, Lu) [36]. On the other hand, many tungstates are self-activated luminescent materials, such as the MWO_4 (M=divalent elements) phases [37,38].

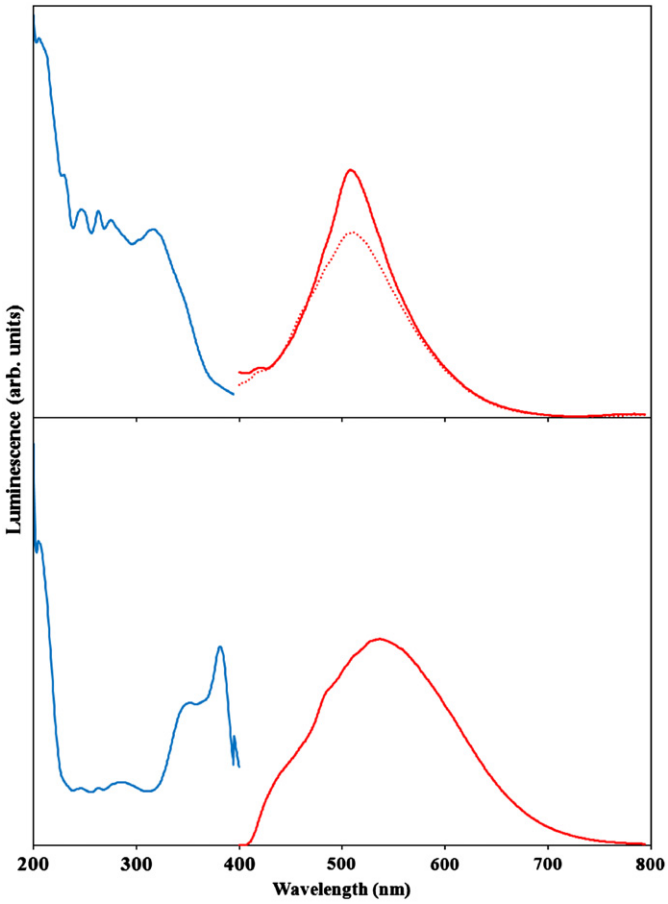

Fig. 8. Room temperature luminescence spectra of Ba_2MgWO_6 (top) and Ba_2ZnWO_6 (bottom). Excitation spectra are shown in blue, emission spectra in red (for Ba_2MgWO_6, the solid red line is for an excitation of 230 nm, the dotted red line is for an excitation of 310 nm). (For interpretation of the references to colour in this figure legend, the reader is referred to the web version of this article.)

4. Conclusion

Single crystals of the cubic double perovskites Ba_2MgWO_6 and Ba_2ZnWO_6 have been grown from potassium carbonate fluxes. Room temperature and low temperature neutron diffraction experiments reveal no phase transitions for these compounds. Luminescence is observed for both materials, with a green emission for Ba_2MgWO_6 and a yellow emission for Ba_2ZnWO_6.

Supplementary information

Powder X-ray diffraction patterns and luminescence spectra are included here. Further details of the crystal structure investigations can be obtained from the Fachinformationszentrum Karlsruhe, 76344 Eggenstein-Leopoldshafen, Germany (fax: +49 7247 808 666; e-mail:crystdata@fiz-karlsruhe.de) on quoting the depository numbers CSD-423033 (Ba_2MgWO_6) and CSD-423034 (Ba_2ZnWO_6).

Acknowledgment

This research was supported by the Heterogeneous Functional Materials for Energy Systems (HeteroFoaM) Energy Frontiers Research Center (EFRC), funded by the U.S. Department of Energy Office of Basic Energy Sciences under Award Number DE-SC0001061. Use of the Spallation Neutron Source is supported by the Division of Scientific User Facilities, Office of Basic Energy Sciences, U.S. Department of Energy, under contract DE-AC05-00OR22725 with UT-Battelle, LLC.

Appendix A. Supplementary material

Supplementary data associated with this article can be found in the online version at doi:10.1016/j.jssc.2011.06.015.

References

[1] E.G. Steward, H.P. Rooksby, Acta. Crystallogr. 4 (1951) 503.
[2] E.J. Fresia, L. Katz, R. Ward, J. Am. Chem. Soc. 81 (1959) 4783.
[3] M.F. Kupriyanov, E.I. Fesenko, Kristallografiya 7 (1962) 451.
[4] I.N. Belyaev, V.S. Filip'ev, E.G. Fesenko, Z. Strukt. Khim. 4 (1963) 719.
[5] E.G. Fesenko, V.S. Filip'ev, M.F. Kupriyanov, Izv. Akad. Nauk SSSR Ser. Fiz. 28 (1964) 669.
[6] V.F. Filip'ev, G.E. Shatalova, E.G. Fesenko, Kristallografiya 19 (1974) 386.
[7] G. Blasse, A.F. Corsmit, J. Solid State Chem. 6 (1973) 513.
[8] H.W. Eng, P.W. Barnes, B.M. Auer, P.M. Woodward, J. Solid State Chem. 175 (2003) 94.
[9] D.D. Khalyavin, J. Han, A.M.R. Senos, P.Q. Mantas, J. Mater. Res. 18 (2003) 2600.
[10] D.D. Khalyavin, J.P. Han, A.M.R. Senos, P.Q. Mantas, Mater. Sci. Forum 455–456 (2004) 30.
[11] C.P. Khattak, D.E. Cox, F.F.Y. Wang, J. Solid State Chem. 17 (1976) 323.
[12] M.C. Viola, M.J. Martínez-Lope, J.A. Alonso, J.L. Martínez, J.M. De Paoli, S. Pagola, J.C. Pedregosa, M.T. Fernández-Díaz, R.E. Carbonio, Chem. Mater. 15 (2003) 1655.
[13] D.E. Cox, G. Shirane, B.C. Frazer, J. Appl. Phys. 38 (1967) 1459.
[14] K.R. Chakraborty, A. Das, P.S.R. Krishna, S.M. Yusuf, S.J. Patwe, S.N. Achary, A.K. Tyagi, J. Alloys Compd. 457 (2008) 15.
[15] D. Reinen, H. Weitzel, Z. Anorg. Allg. Chem. 424 (1976) 31.
[16] G. Madariaga, A. Faik, T. Breczewski, J.M. Igartua, Acta Crystallogr. B: Struct. Sci. 66 (2010) 109.
[17] C.P. Khattak, J.J. Hurst, D.E. Cox, Mater. Res. Bull. 10 (1975) 1343.
[18] B.N. Sun, R. Boutellier, P. Sciau, E. Burkhardt, V. Rodriguez, H. Schmid, J. Cryst. Growth 112 (1991) 71.
[19] A. El Abed, E. Gaudin, H.-C. zur Loye, J. Darriet, Solid State Sci. 5 (2003) 59.
[20] K.E. Stitzer, A. El Abed, J. Darriet, H.-C. zur Loye, J. Am. Chem. Soc. 123 (2001) 8790.
[21] K.E. Stitzer, M.D. Smith, H.-C. zur Loye, J. Alloys Compd. 338 (2002) 104.
[22] R.B. Macquart, M.D. Smith, H.-C. zur Loye, Cryst. Growth Des. 6 (2006) 1361.
[23] I.P. Roof, M.D. Smith, H.-C. zur Loye, J. Chem. Crystallogr. 40 (2010) 491.
[24] I.P. Roof, M.D. Smith, H.-C. zur Loye, Solid State Sci. 12 (2010) 1941.
[25] S. Obbade, S. Yagoubi, C. Dion, M. Saadi, F. Abraham, J. Solid State Chem. 174 (2003) 19.
[26] S. Obbade, C. Dion, E. Bekaert, S. Yagoubi, M. Saadi, F. Abraham, J. Solid State Chem. 172 (2003) 305.
[27] SMART Version 5.625, SAINT+ Version 6.22, and SADABS Version 2008/1, Bruker Analytical X-Ray Instruments, Madison, WI, USA, 2008.
[28] G.M. Sheldrick, Acta Crystallogr. A: Found. Crystallogr. 64 (2008) 112.
[29] A.C. Larson, R.B. von Dreele, General Structure Analysis System (GSAS), Los Alamos National Laboratory, Los Alamos, NM, USA, 1990.
[30] B.H. Toby, J. Appl. Crystallogr. 34 (2001) 210.
[31] S.J. Patwe, S.N. Achary, M.D. Mathews, A.K. Tyagi, J. Alloys Compd. 390 (2005) 100.
[32] M.J. Martínez-Lope, J.A. Alonso, M.T. Casais, M.T. Fernández-Díaz, Eur. J. Inorg. Chem. (2002) 2463.
[33] J.H.G. Bode, A.B. van Oosterhout, J. Lumin. 10 (1975) 237.
[34] F.A. Kröger, Some Aspects of Luminescence of Solids, Elsevier, New York, 1948.
[35] G. Blasse, Prog. Solid State Chem. 18 (1988) 79.
[36] G. Blasse, A. Bril, J. Solid State Chem. 2 (1970) 291.
[37] G. Blasse, G.J. Dirksen, M. Hazenkamp, J.R. Günter, Mater. Res. Bull. 22 (1987) 813.
[38] A.A. Blistanov, B.I. Zadneprovskiĭ, M.A. Ivanov, V.V. Kochurikhin, V.S. Petrakov, I.O. Yakimova, Crystallogr. Rep. 50 (2005) 284.